

# Pseudo-affine behaviour of collagen fibres during the uniaxial deformation of leather

C. BOOTE

*Department of Optometry and Vision Sciences, University of Cardiff,  
Redwood Building, King Edward VII Avenue, Cardiff CF10 3NB, UK  
E-mail: bootec@cardiff.ac.uk*

E. J. STURROCK, G. E. ATTENBURROW

*British School of Leather Technology, University College Northampton,  
Park Campus, Northampton NN2 7AH, UK*

K. M. MEEK

*Department of Optometry and Vision Sciences, University of Cardiff,  
Redwood Building, King Edward VII Avenue, Cardiff CF10 3NB, UK*

Chromium tanned bovine leather has been dried under uniaxial strain and its collagen fibre distribution examined using high-angle X-ray diffraction. Microstructural modelling of the fibre kinematics showed that under large-strain deformation (30%) the fibres behave in a pseudo-affine manner. At decreasingly lower strains the fibre re-orientation is seen to progressively deviate from the pseudo-affine prediction; an observation which can be understood in terms of a combination of fibre-fibre adhesion and changes in fibre substructure. The material was also subjected to mechanical testing and tensile data is presented here which indicates how fibre orientation affects tensile modulus. This work represents the first quantitative microstructural model for collagen fibre distribution in strained leather. © 2002 Kluwer Academic Publishers

## 1. Introduction

Since tanneries purchase hides by weight but sell leather by area there is considerable interest in maximising area yield during processing. Maintaining leather in a stretched condition during drying is a potentially effective route to achieving this [1]. However, there is evidence that this process can adversely affect the properties of the finished product [2], particularly its stiffness [3] and strength [4]. The link between changes in tensile properties and microstructure of leather is currently poorly understood, and the volume of published work on the quantitative study of leather structure is limited.

Chromium tanned leather consists essentially of an interwoven network of fibres composed of a chemically cross-linked form of collagen, a triple-helical protein notable for its mechanical strength and thermal/chemical stability. Electron microscopy [5, 6] has revealed a hierarchy of structure within leather collagen fibres. Individual rod-like collagen molecules are assembled into fibrils, which then group together in roughly parallel arrays to form bundles and ultimately individual fibres. Collagen confers tensile reinforcement upon biological tissues [7]. The directions of fibre orientation are closely associated with the directions in which a tissue is able to withstand tensile stress, and hence are responsible for its general mechanical properties. This relationship has been studied in a diverse

range of tissues including leather (Sturrock *et al.* [3]), cartilage (Aspden *et al.* [8]), and aorta (Purslow [9]). Collagen fibres within a tissue can rotate in response to an imposed unidirectional strain, and thus alter its tensile properties. Recently we have shown that the bending stiffness of bovine leather dried under uniaxial strain shows a marked dependence on the angle to the strain axis and the degree of applied strain, and that this can be understood in terms of changes in the fibre distribution [3]. Thus there is considerable worth in obtaining quantitative information about the kinematics of collagen fibre distribution during the deformation of leather.

Several methods have previously been adopted to investigate fibre distribution in leather, including X-ray diffraction [3], electron microscopy [6, 10] and microwave methods [11]. The benefits of X-ray diffraction applied to leather are that it offers rapid quantitative assessment of the collagen fibre distribution *in situ*, and can be used to sample a large enough area to give a representative view of the fibre distribution within a macroscopic specimen.

Microstructural modelling of fibre kinematics during deformation has been performed on a number of collagenous biological systems such as skin [12, 13] and aortic valve [14]. In general these tissues have been broadly classified as 'affine' or 'non-affine', where in the case of affine materials the measured change in

fibre distribution can be predicted on the basis that the microscopic fibre motion follows the macroscopic applied deformation. A microstructural model for leather, based on an idealised two-dimensional fibre network, has been recently proposed to describe the non-linear modulus increase of leather dried under increasing uniaxial strain [15]. However, there is currently no published work on the quantitative modelling of fibre distribution in leather. We present here a model for the fibre kinematics of uniaxially pre-strained leather, based on a pseudo-affine model originally developed for synthetic polymers, and use X-ray diffraction to test the affine assumption. The consequences of the observed changes in fibre orientation distribution for tensile modulus are also explored.

## 2. Theory

### 2.1. Affine model

In 1951 Crawford and Kolsky [16] used birefringence data to show that molecular reorientation during the extension of polyethylene does not follow rubber elasticity theory but rather could be predicted using an affine model of the reorientation of hypothetical rod-like crystallites. More recently affine deformation theory has also been applied to model the reorientation of

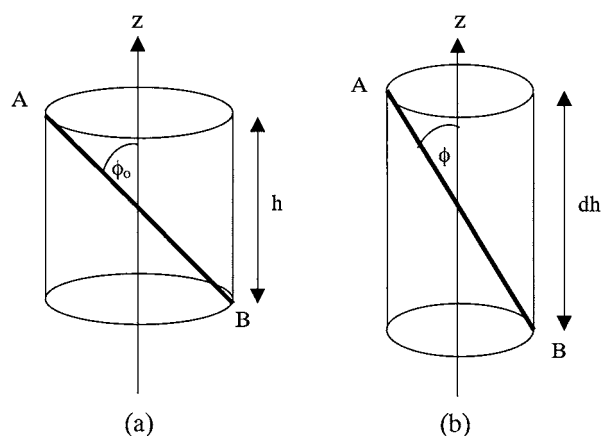


Figure 1 Rotation of a collagen fibre.

slip planes during large-strain deformation of the same polymer [17].

In this paper we report on the novel application of the affine deformation model to predict the alignment of collagen fibres during the uniaxial deformation of leather. Consider a fibre represented by the line AB (see Fig. 1a), inclined at an angle  $\phi_0$  to the  $z$ -axis, and fully enclosed by a cylinder of height  $h$ . Upon deformation in the  $z$  direction (see Fig. 1b), the cylinder extension is such that the inclination angle becomes  $\phi$  and the volume of the cylinder is conserved, so that:

$$\tan(\phi) = d^{-3/2} \tan(\phi_0) \quad (1)$$

where  $d$  is the stretch ratio. The number of fibres per degree inclination is then,

$$B = B_0 \frac{d^{3/2}}{1 + (d^3 - 1) \sin^2\left(\frac{\phi}{57.3}\right)} \quad (2)$$

where  $B_0$  is the fibre distribution before stretching (i.e.,  $d = 1$ ).

### 2.2. High-angle X-ray fibre diffraction

As for many biological tissues, the collagen fibrils within the fibres of leather may be described as being structurally similar to a smectic A liquid crystal mesophase [18]. That is to say the rod-like molecules are oriented with their long axes roughly parallel, but have no long-range periodic order. The high-angle diffraction pattern from leather therefore consists of only a single  $\sim 12 \text{ \AA}$  intermolecular reflection, arising from the short-range order produced by molecules excluding each other from the space they occupy. This is shown in Fig. 2.

Consider a collimated X-ray beam, of wavelength  $\lambda$ , incident on a single collagen fibre. Let the amplitude and phase of scattered X-rays be represented by  $F(\mathbf{K})$ , where  $\mathbf{K}$  is related to the scattering angle,  $2\theta_B$ , by,

$$|\mathbf{K}| = (4\pi/\lambda) \sin \theta_B \quad (3)$$

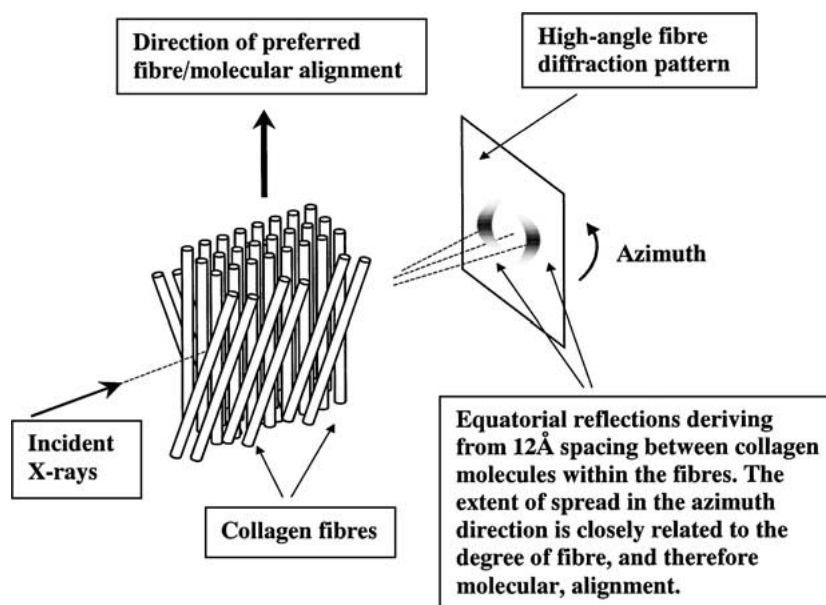


Figure 2 High-angle X-ray diffraction of collagen fibres.

For an assembly of  $N$  fibres the resultant scattered intensity is given by,

$$I(\mathbf{K}) = \sum_{j=1}^N F_j(\mathbf{K})F_j^*(\mathbf{K}) + \sum_{j \neq k} \sum_{k=1}^N F_j(\mathbf{K})F_k^*(\mathbf{K}) \times \exp[-i(\mathbf{r}_j - \mathbf{r}_k) \cdot \mathbf{K}] \quad (4)$$

where  $\mathbf{r}_j$  defines the position of the  $j$ th fibre. However, since the fibres in leather are essentially randomly interwoven (i.e., random  $\mathbf{r}_j$ ), the second term tends to zero for large  $N$ , yielding,

$$I(\mathbf{K}) = \sum_{j=1}^N F_j(\mathbf{K})F_j^*(\mathbf{K}) \quad (5)$$

Hence, the diffraction pattern from an assembly of leather collagen fibres is simply the sum of the intensities scattered by the individual fibres, and interference between fibres may be ignored. It follows that, to a first approximation, the X-ray intensity will be proportional to the number of aligned fibres, and we may define the angular fibre distribution  $B(\phi)$  as,

$$B(\phi) \cong I(\phi') \quad (6)$$

where  $\phi'$  is the azimuth angle at the detector and is equal to  $\phi + 90^\circ$  (i.e., a fibre is assumed to diffract the X-ray beam in a plane normal to its long axis).

### 3. Materials and methods

A wet blue chromium tanned bovine hide was obtained from a UK tannery. In brief, the term “wet blue” refers to a hide that has been fully preserved and tanned using chromium salts, to leave material essentially comprising of a non-biodegradable cross-linked collagen network [19]. The hide was shaved to a uniform thickness of  $\sim 1.7$  mm and cut down the backbone, with one side to be used for controls and the other for stretching. Three rectangular shaped samples ( $15 \text{ cm} \times 32 \text{ cm}$ ) were cut from the sampling area on each side. The

strained samples were stretched along their long axis (parallel to the backbone) by 10, 20 or 30% using an Instron 1122 testing machine, and left to dry for 48 hours. On removal from the grips of the machine it was found that the stretch imparted before drying had been retained.

Seven rectangular ( $15 \text{ mm} \times 5 \text{ mm}$ ) specimens were cut from each pre-strained sample and its respective control. The specimens were cut from different regions of each piece in order to give a representative view of fibre distribution over the whole sample region such that the long specimen axis coincided with the pre-strain axis. High-angle X-ray diffraction patterns were obtained on station 14.1(b) at the Daresbury Synchrotron Radiation Source, using a wavelength of  $1.488 \text{ \AA}$  and a square beam cross-section of  $0.5 \text{ mm} \times 0.5 \text{ mm}$ . Specimens were oriented with their largest face normal to the incident beam and with the strain axis in the vertical direction. Relative normalised intensities over the azimuth range:  $0^\circ \leq \phi' \leq 180^\circ$  were obtained as described previously [20] and averaged over the seven specimens for 0, 10, 20 and 30% pre-strains respectively.

Mechanical test pieces ( $8 \text{ cm} \times 1.7 \text{ cm}$ ) were cut, in increments of  $15^\circ$ , at various angles,  $\phi$ , ( $0-90^\circ$ ) to the pre-strain axis. These pieces were subjected to tensile testing at a rate of  $5 \text{ mm/min}$  using the Instron 1122 machine with a  $5 \text{ kN}$  load cell and an initial jaw separation of  $5 \text{ cm}$ . Their stress-strain relationship was determined and initial tensile moduli were calculated.

## 4. Results and discussion

### 4.1. Fibre orientation distribution

Fig. 3 shows the angular X-ray intensity profiles for chromium tanned bovine leather subjected to pre-strains of 0, 10, 20 and 30%. The increasing sharpness and height of the peaks at  $\phi' = 0$  and  $180^\circ$  shows that the fibres become increasingly oriented along the pre-strain axis ( $\phi' = 90^\circ$ ) as the material is deformed. Such re-alignment of fibres on stretching has been observed for other collagenous materials [13, 14, 21]. Increasing the strain by 10% produces a remarkably consistent relative change in fibre alignment. The variation of intensity with angle for the control indicates a non-uniform

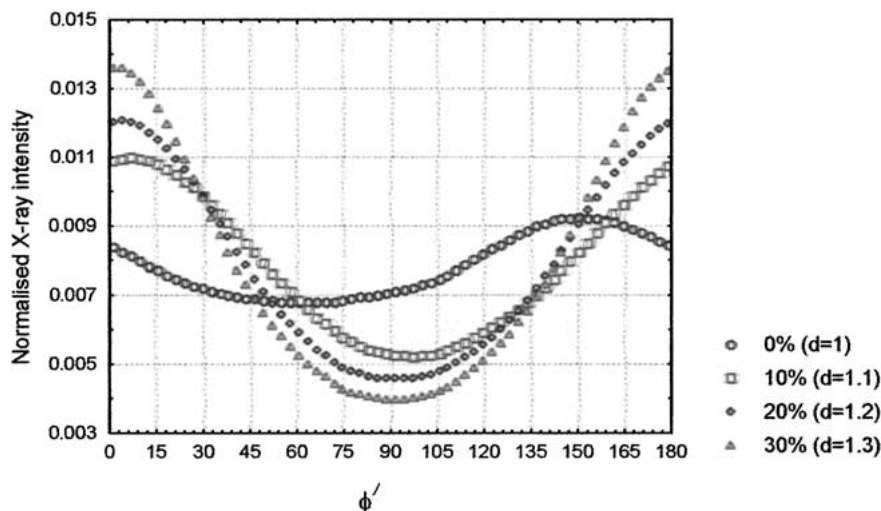


Figure 3 Normalised angular X-ray intensity distributions from chromium tanned bovine leather dried under uniaxial strains of 0, 10, 20 and 30%. The pre-strain axis corresponds to  $\phi' = 90^\circ$ .

fibre orientation distribution and this is in agreement with the work of Osaki [22], who demonstrated by microwave methods that in undeformed leather there is a position dependent preferred fibre run. The X-ray data shows that the undeformed distribution follows a Gaussian shape (as does the stretched material) and indicates that the predominant fibre orientation for our chosen sampling area on the hide is around  $\phi = 30^\circ$ ; a value which we found to be highly reproducible for this region of our hide, though significant variation was found both within and between individual X-ray specimens.

Fig. 4 shows the fibre distributions after deformation,  $B$ , determined by X-ray diffraction and calculated using the pseudo-affine model of Equation 2. Only data in the range  $0^\circ \leq \phi \leq 90^\circ$  are shown, since the distributions are symmetrical about their respective peaks due to cylindrical averaging of collagen molecules about the fibre axis. It is evident from Fig. 4c that the pseudo-affine model can predict the distribution of fibres after 30% uniaxial deformation. At 20% and 10% pre-strains the experimental data is seen to progressively deviate

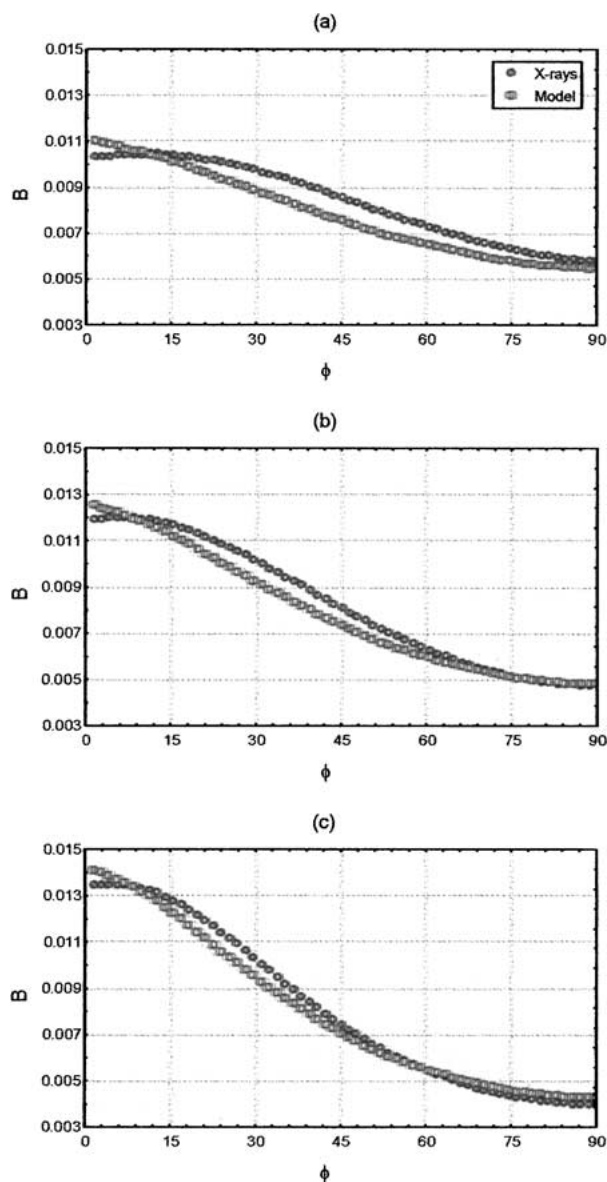


Figure 4 Collagen fibre distributions after deformation  $B$  for leather dried under pre-strains of: (a) 10%, (b) 20% and (c) 30%. The pre-strain axis corresponds to  $\phi = 90^\circ$ .

from the model, although to a good approximation the behaviour of fibres at 20% can still be classified as affine.

Fig. 4a shows that at 10% pre-strain the deviation of the fibre distribution from the pseudo-affine prediction becomes significant. Non-affine fibre behaviour has been demonstrated in other collagenous tissues [13, 14] and partly accounted for by the inherently composite nature of biological materials. For example, the systematic deviation from affine behaviour of collagen fibres in porcine skin has been attributed to a non-affine relationship between the collagen and the ground substance [14], where “ground substance” refers to the skin components other than fibrillar collagen. However since most of the interfibrillar material present in raw bovine hide is removed by the tanning process chromium tanned leather is not a true composite material, and for the purposes of fibre modelling may be considered to consist essentially of pure collagen. In fact whilst tanned leather may also contain some elastin fibres, their content in bovine hide is relatively low at around 0.20%–0.34% [23]. Elastin is found by optical microscopy to be almost exclusively situated in the upper papillary or grain layer as a network of fine fibres and survives the leathernaking process, although its fibrous network is considerably disrupted [24]. Elastin after drying is below its glass transition temperature [25] and as such may be expected to make a minor contribution towards the stiffness of the grain layer. The grain/corium ratio for the samples tested in this work was 1 : 2.75.

During the low-strain deformation of leather the systematic deviation of the X-ray measurements from affine theory is likely due to two main factors. Firstly, while the pseudo-affine model assumes ‘free-rotation’ of all fibres, the collagen fibres in leather in fact form an entangled network [5, 6] and there is evidence for the formation of inter-fibre adhesion bonds during drying of wet material [26]. Furthermore, the chromium tanned material used in our studies was not fatliquored, a process that is known to minimise inter-fibre adhesion during drying [10]. Secondly, it is important to remember that the high-angle diffraction pattern from leather derives from the regular lateral separation of individual collagen molecules. Therefore changes in orientation on any level within the hierarchy of fibre structure will affect the angular distribution of intensity in a leather high-angle diffraction pattern: changes in the alignment of molecules, fibrils and fibres will be indistinguishable. The re-orientation of fibrils within fibres has been observed in other tissues [13], and it is likely that this can also occur within leather fibres that are either already fully aligned or experiencing resistance to movement due to inter-fibre adhesion.

## 4.2. Mechanical properties

A typical set of stress-strain relationships (for material pre-strained by 30%) is shown in Fig. 5. Ultimate properties vary markedly with test angle and are similar to those discussed in [4]. Of interest here are the low strain portions of the curves (Fig. 6) whose slope (measured as a secant between 0 and 2% strain) was used to

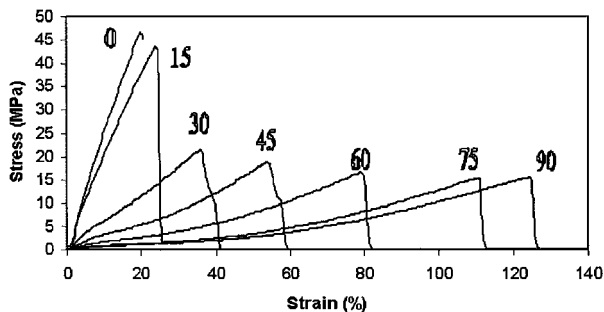


Figure 5 Stress-strain curves for leather dried under 30% pre-strain. Numbers alongside curves indicate the test direction ( $\phi^\circ$ ).

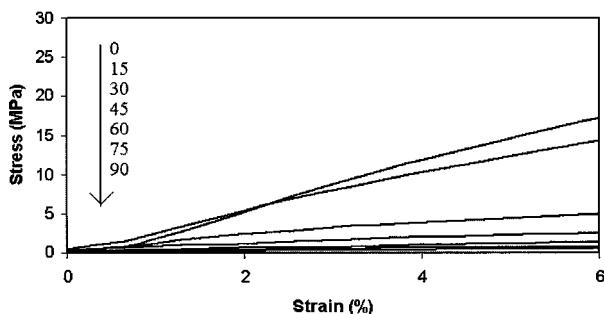


Figure 6 Shows low strain region of curves presented in Fig. 5. The test directions ( $\phi = 0^\circ$ – $90^\circ$ ) are indicated by the arrow.

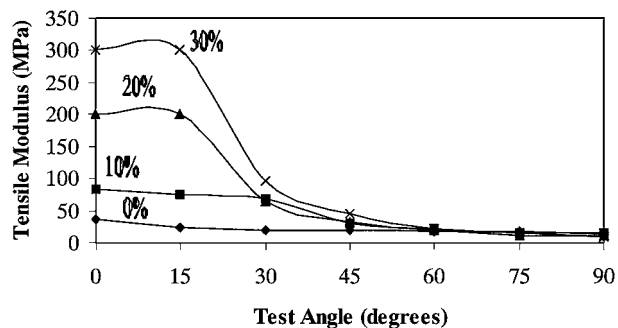


Figure 7 Initial tensile modulus,  $E_\phi$ , plotted against test angle,  $\phi$ . The applied pre-strain (%) is indicated by each curve.

define a tensile modulus. Fig. 7 shows the variation of this tensile modulus ( $E_\phi$ ) with test angle ( $\phi$ ). It can be seen that the unstretched material has  $E_\phi \sim 25$  MPa for  $\phi = 15$ – $90^\circ$  increasing to 40 MPa at  $\phi = 0^\circ$ . The effect of drying the leather under strain is seen to substantially increase  $E_\phi$  for  $\phi = 0^\circ$  and  $15^\circ$  with the amount of increase dependent on the strain applied during drying. Above  $15^\circ$ ,  $E_\phi$  falls but remains greater than that of the unstretched control until  $\phi = 60^\circ$ . At the higher angles ( $\phi = 75^\circ$  and  $\phi = 90^\circ$ )  $E_\phi$  values for stretched material fall below those of the undeformed control. It is clear that for material stretched by 30% the degree of anisotropy developed is large ( $E_0/E_{90} = 30$ ). Our hypothesis has been that the changes in  $E_\phi$  caused by drying under strain are due to changes in the angular distribution of the constituent fibres and so it is instructive to compare the data presented in Figs 4 and 7. This is done in Fig. 8 where the X-ray intensity relative to the control is plotted against the tensile modulus relative to the control. It would seem that the modulus distribution is not related to the fibre orientation distribution

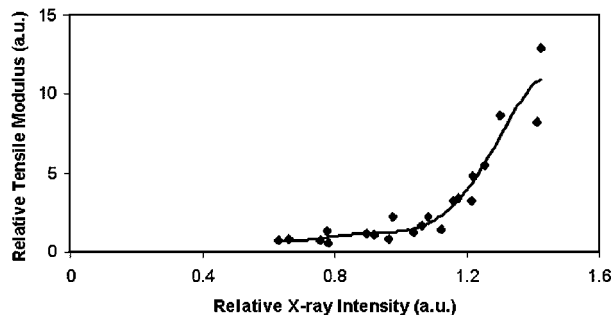


Figure 8 Relative X-ray intensity plotted against relative tensile modulus.

in any simple linear fashion and it appears that tensile modulus increases ever more rapidly as more fibres are oriented along the test axis. When the X-ray intensity is low the implication is that not many fibres are oriented at that angle. The modulus increases at  $15^\circ$  and  $0^\circ$  are the most pronounced. The simple model put forward in an earlier publication [15] provided an insight into deformation mechanisms responsible for tensile modulus increases along the pre-strain axis. In its present form this model cannot describe modulus changes in other directions.

## 5. Conclusions

The fibre kinematics of chromium tanned bovine leather dried under large uniaxial strain appears to be affine. At pre-strains of 20–30% good agreement is found between the fibre distribution estimated by X-ray diffraction and that predicted using the geometrical pseudo-affine model. Systematic deviation of the experimental data from the model at strains of  $<20\%$  may be accounted for by a combination of fibre-fibre interactions and fibril re-organisation within fibres. This work represents the first quantitative model for collagen fibre distribution in leather, and will help to better our understanding of the microstructural basis for changes in the tensile properties of leather.

## Acknowledgements

The authors would like to thank Dr Richard Newton for his advice concerning the analysis of X-ray data. This work was funded by a grant from the EPSRC (GR/M77451/M77444).

## References

1. D. M. WRIGHT and G. E. ATTENBURROW, in XXIII IULTCS Congress Proceedings, London, UK, 1977, p. 686.
2. R. DANIELS, *World Leather* (1993) 251.
3. E. J. STURROCK, G. E. ATTENBURROW, C. BOOTE and K. M. MEEK, *J. Soc. Leath. Tech. Chem.* **86**(1) (2002) 6.
4. M. G. OTUNGA and G. E. ATTENBURROW, in Proceedings of the 11th International Conference on Deformation, Yield and Fracture of Polymers, Cambridge, UK, April 2000 (IOM Communications) p. 397.
5. G. REICH, *J. Soc. Leath. Tech. Chem.* **83** (1999) 63.
6. K. T. W. ALEXANDER, A. D. COVINGTON, R. J. GARWOOD and A. M. STANLEY, in XXII IULTCS Congress Proceedings, Porto Alegre, Brazil, November 1993.
7. D. W. L. HUKINS and R. M. ASPDEN, *TIBS* **10**(7) (1985) 260.
8. R. M. ASPDEN, Y. E. YARKER and D. W. L. HUKINS, *J. Anat.* **140** (1985) 371.
9. P. P. PURSLOW, *J. Biomech.* **16**(11) (1983) 947.

10. A. M. STANLEY, *Micr. Anal.* (1992) 25.
11. S. OSAKI, M. O. YAMADA, A. TAKAKUSU and K. MURAKAMI, *Cell. Mol. Biol.* **39** (1993) 673.
12. Y. LANIR, *J. Biomech.* **16** (1983) 1.
13. D. G. HEPWORTH, A. STEVEN-FOUNTAIN, D. M. BRUCE and J. F. V. VINCENT, *ibid.* **34** (2001) 341.
14. K. L. BILLIAR and M. S. SACKS, *ibid.* **30**(7) (1997) 753.
15. D. M. WRIGHT and G. E. ATTENBURROW, *J. Mater. Sci.* **35** (2000) 1353.
16. S. M. CRAWFORD and H. KOLSKY, *Proc. Phys. Soc. B* **64** (1951) 119.
17. S. J. K. RITCHIE, *J. Mater. Sci.* **35** (2000) 5829.
18. D. W. L. HUKINS and J. WOODHEAD-GALLOWAY, *Mol. Cryst. Liq. Cryst.* **41** (1977) 33.
19. G. E. ATTENBURROW and D. M. WRIGHT, *J. Amer. Leather Chemists Assoc.* **89** (1995) 391.
20. R. H. NEWTON and K. M. MEEK, *Inv. Opth. Vis. Sci.* **39** (1998) 1125.
21. X. MARKENSCOFF and I. V. YANNAS, *J. Biomech.* **12** (1979) 127.
22. S. OSAKI, *Anat. Rec.* **254** (1999) 147.
23. C. DEASY and J. J. TANCOSUS, *J. Amer. Leath. Chem. Assoc.* **66** (1971) 545.
24. W. T. RODDY and F. O'FLAHERTY, *ibid.* **33** (1938) 512.
25. H. BATZER and U. T. KRIEBICH, *Polymer Bulletin* **5** (1981) 585.
26. P. KRONICK, A. PAGE and M. KOMANOWSKY, *J. Amer. Leath. Chem. Assoc.* **88** (1993) 178.

*Received 14 August 2001  
and accepted 17 April 2002*